

# STRUCTURAL, OPTICAL AND ELECTRICAL PROPERTIES OF NANOSTRUCTURED ZnO THIN FILMS FOR HYBRIDE PHOTOVOLTAIC CELLS

C. Tăzlaşoanu, M. Radu, V. Covlea, Larisa Magherusan, L. Ion, S. Antohe  
University of Bucharest, Faculty of Physics, P.O. Box MG-11, Magurele, Ilfov,  
077125, ROMANIA

## Abstract

*Structural, electrical and optical characterizations of nanostructured ZnO thin films used as photosensitized electrodes in photovoltaic cells applications are reported. Nanostructured ZnO thin films were deposited on optical glass substrates by pulsed-laser deposition (PLD), their structure and morphology being optimized for photovoltaic applications. Structural analysis of the samples by X-ray diffraction revealed that the films consist of a hexagonal-close-packed wurtzite type phase ZnO, (001) preferentially oriented in the growth direction. The ZnO films are highly transparent in visible region of solar spectrum, and exhibit electrical resistivities in the range  $10^{-4} - 10^{-2} \Omega \cdot m$*

## 1. INTRODUCTION

An extensive research work has been performed in the last decade in the field of transparent conductive oxide (TCO) films, because of their peculiar physical properties (large bandgaps, typically larger than 3 eV, and consequently high optical transparency in a spectral region extending from near-infrared to ultra-violet, associated with low resistivities ( $\rho < 10^{-2} \Omega \cdot m$ ). Due to those properties, TCO films are well suited for applications in the field of thin film solar cells, optoelectronics, transparent electrodes, selective coatings, etc. Several materials have been widely studied, such as Sn-doped  $In_2O_3$  [1-3] (ITO), ZnO [4-6],  $SnO_2$  [7,8], using various deposition techniques. Among them, ZnO gained a special attention because it is a non-toxic, relatively more abundant and inexpensive material. Also, its direct bandgap, a large optical absorption coefficient and a very large exciton binding energy (60 meV) [9] are particularly interesting for optoelectronic applications. TCO films based on ZnO have been prepared with resistivities as low as  $10^{-5} \Omega \cdot m$  (see, for example, [10] and references therein).

Among the deposition techniques used for obtaining good quality ZnO films, pulsed laser deposition (PLD) was proved to be a versatile one, well suited for making thin films with complex chemical compositions and various structural and morphological characteristics. The main thing about PLD is that it provides good control over several parameters during deposition. In this work, an investigation of structural, electrical and optical properties of ZnO thin films deposited by PLD and optimized for use in hybrid organic/inorganic photovoltaic cells, has been performed. It is organized as follows: in the next section details about preparation conditions and experimental methods used for film characterization are given. The obtained results, regarding the structure, electrical and optical properties of the films, are discussed in the third section. The fourth section summarizes the main conclusions of this study.

## 2. EXPERIMENTAL PROCEDURES

ZnO thin films were synthesized by pulsed KrF\* ( $\lambda = 248$  nm and  $\tau_{FWHM} \approx 7$  ns) laser ablation of ZnO targets on optical glass. The reaction chamber was evacuated to a residual gas pressure below  $10^{-4}$  Pa. Data regarding preparation conditions of the films analyzed in this paper are collected in table I. The crystallinity of the films was characterized by X-ray diffraction (XRD), using a  $\theta$ - $2\theta$  diffractometer. XRD spectra were recorded by using Cu- $K_{\alpha}$  line,  $\lambda = 1.54178$  Å. Line profiles were recorded in a step-scanning regime, with  $\Delta(2\theta) = 0.01^{\circ}$ .

**Table I.** - PLD deposition conditions and parameters of obtained thin films

Sample	Target	Substrate	Deposition Temperature [°C]	Oxygen Pressure [Pa]	$D_{eff}^*$ [nm]	Film Thickness [nm]
ZO1	ZnO	Optical glass	400	6.5	34	248
ZO2	ZnO:Al(2%)	Optical glass	400	6.5	61	296
ZO3	ZnO	Optical glass	400	1.3	32	460

\* Crystallite size, as determined from (002) XRD peak with Scherrer formula, eq. (1).

Optical properties of the films were characterized by performing transmittance and photoluminescence (PL) measurements. The photoluminescence was recorded at room temperature, with excitation at 370 nm. Transmittance data were recorded with a Perkin-Elmer Lambda 35 spectrometer.

Electrical measurements were performed using a Keithley 2400 Source Meter and a Keithley 6517 electrometer. The films were placed in a He closed cycle cryostat with sample in vacuum (residual pressure was below  $10^{-2}$  Pa), having four quartz windows for optical access to the sample. The temperature of the analyzed samples was varied between 20 K and 300 K. The sheet resistance was measured in a four-points configuration.

## 3. EXPERIMENTAL RESULTS and DISCUSSIONS

### 3.1 Crystalline structure

Structural analysis of the samples by X-ray diffraction revealed that the films consist of a hexagonal-close-packed wurtzite type phase ZnO, (001) preferentially oriented in the growth direction (see figure 1a). This type of packing, with the c-axis oriented perpendicularly to the film surface, occurring even at low substrate temperature, seems to be a peculiarity of ZnO.

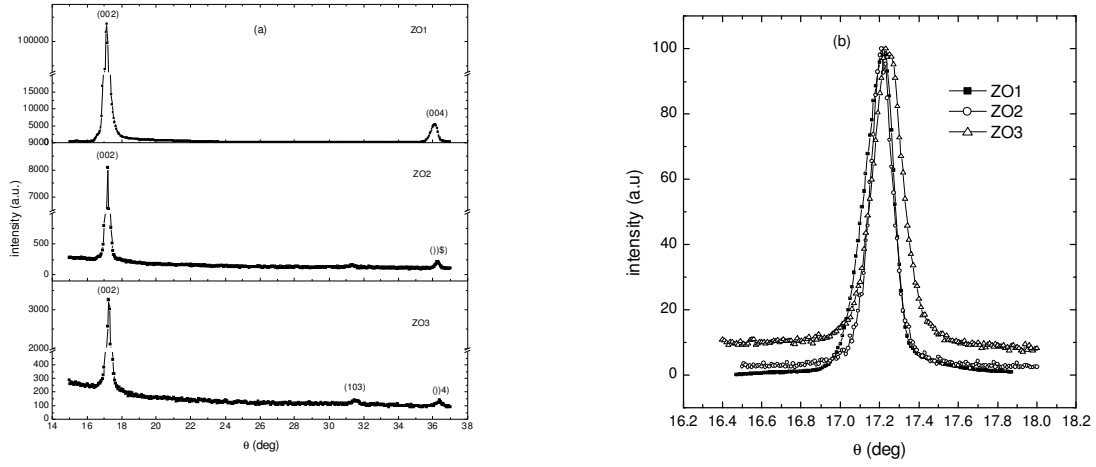


**Figure 1.** Experimental X-ray diffraction pattern of analyzed ZnO samples (a) and an enlargement of (002) normalized peak (b).

From the full width at half maximum,  $\delta$ , of the (002) XRD peak (see figure 1b), the size of the crystallites, (coherence lengths) was determined for ZO1, ZO2 and ZO3 samples using the well-known Scherrer formula:

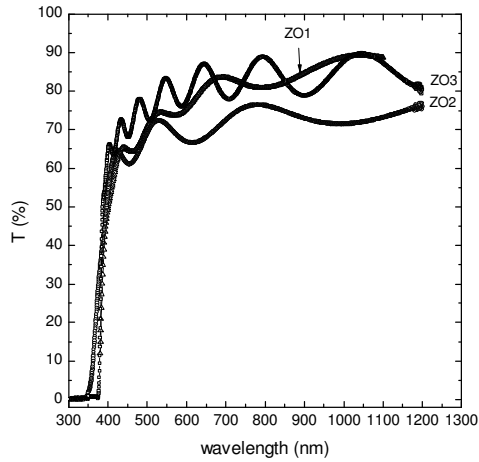
$$D_{eff} = \frac{0.9\lambda_x}{\delta \cos \theta_0}, \quad (1)$$

where  $\lambda_x$  is the X-ray wavelength and  $\theta_0$  is the angle where the peak occurs. The values are indicated in table I. There is a large difference between the film thickness values and the crystallite sizes in the growth direction. It can be explained by the fact that the film structure is rather granular, not columnar. Based on the fact that the broadening of the (002) peak is induced by the crystallites with smallest size in the growth direction, the small values of the crystallite size, as determined from equation 1, may also be due to the crystallites formed in the early stage of the film growth.

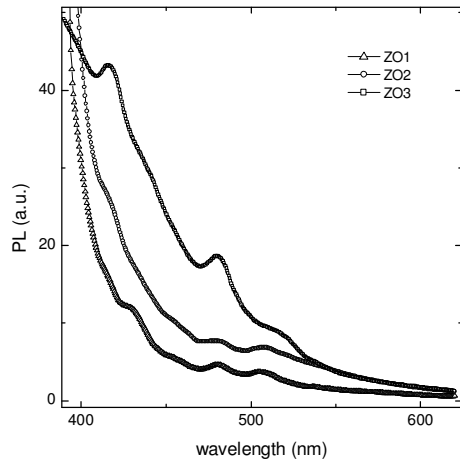
### **3.2 Optical properties**

Figure 2 shows transmission spectra of the samples listed in table I. The films ZO1 and ZO3 exhibit a relatively high transmittance (>75%) in the visible region, while the transmittance of the sample ZO2 is somewhat lower. A sharp fundamental absorption edge can be observed in all cases at 378 nm (3.28 eV).

Photoluminescence spectra are shown in figure 3. The same features are present in all recorded spectra. All the samples show emission from deep levels, at about 518 nm (2.39 eV, “green band”), generally attributed to a shallow donor-deep acceptor pair transition [11,12]. There are two peaks, at about 416 nm (2.98 eV) and 480 nm (2.58 eV) with increasing intensity from ZO1 to ZO3 sample. Since ZO3 sample has the most pronounced oxygen deficiency (see table I), it seems that the above mentioned emission peaks are related to defects resulting from that condition.



**Figure 2.** Optical transmittance recorded for the three samples in table I.



**Figure 3.** Photoluminescence spectra of the ZnO films listed in table I.

### **3.3 Electrical properties**

The temperature dependence of the resistivities of the analyzed samples is shown in figure 4. Hall measurements (not shown) revealed that free carrier density is practically constant in the temperature range (50 K – 320 K) for all samples. It follows that the observed temperature dependence of the resistivity is in fact due to the mobility of the free carriers. It was argued [10,13] that in TCO films free carriers are mainly scattered by ionized impurities and, at high enough temperature, by phonons. In the case of ZnO, piezoelectric scattering by acoustic phonons and scattering by optical phonons must be taken into account, although optical phonon contribution should be dominant at temperatures much higher than room temperature. The piezoelectric scattering by acoustic phonons results in a temperature dependence of the mobility of the form  $\mu_L \propto \frac{1}{T}$  [14]. This is the observed behavior at temperatures larger than 130 K. At lower temperature the resistivity tends to saturate. In that range free carriers are mainly scattered by ionized and, at very low temperature, by neutral impurities. TCO films contain high densities

of point defects, acting as donors or acceptors. For instance, high-energy electron irradiation experiments [15] and theoretical predictions [16] suggest that interstitial zinc is the native shallow donor in ZnO, located at 0.03 eV below the conduction band edge. Also,  $Al_{Zn}$  acts as a shallow donor, with an ionization energy of 0.05 eV [16]. In degenerate electronic systems, the mobility is practically temperature independent in both ionized and neutral impurity scattering mechanisms (see equations 5 and 6) in Ref. [10]).

In figure 5 external quantum efficiency (EQE) of a photovoltaic cell ZnO/CuPc/Au is shown. The cell uses a ZnO sample of ZO3 type as transparent electrode. A copper-phthalocyanine (CuPc) film, 600 nm thick, is used as absorbing layer. CuPc film was vacuum sublimated onto ZnO TCO at 400 °C ( $10^{-3}$  Pa residual pressure, 150 °C substrate temperature) and thermally treated in vacuum at 100 °C for 10 min. A 300 nm thick gold film was subsequently vacuum sublimated as back-electrode. The cell performance is rather modest, mainly due to the charge transfer at ZnO/CuPc interface. Work is in progress, to improve the performance of such structures.

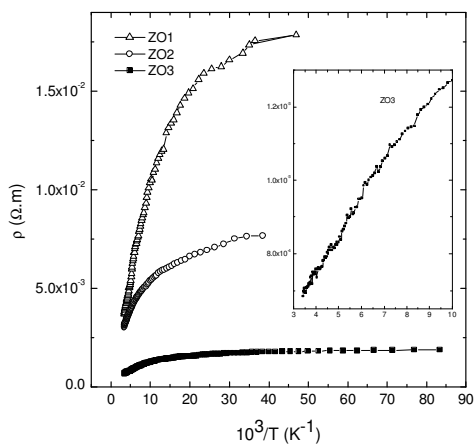


**Figure 4.** Temperature dependence of electrical resistivity. The high temperature region in the case of ZO3 sample is shown in inset.

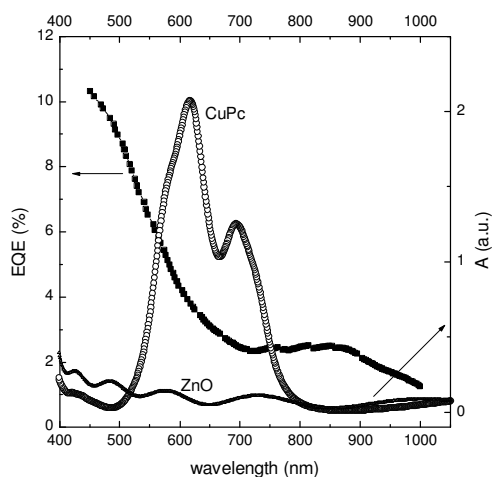


**Figure 5.** External quantum efficiency of the ZnO/CuPc/Au photovoltaic structure. For reference, absorption spectra of CuPc and ZnO films are also shown.

## CONCLUSIONS

Structural, electrical and optical characterizations of PLD deposited ZnO thin films, intended for use in solar cell applications, were performed. The films contain a wurtzite phase and show a preferential orientation, with c-axis perpendicular to the substrate. Optical transmittance is above 75% in the visible region, being a little smaller in the case of Al-doped sample. Temperature dependence of the resistivity of the films was recorded. Extrinsic doping with Al has proved to be less efficient than intrinsic doping:  $3 \times 10^{-3} \Omega \cdot \text{m}$  for ZnO:Al (sample ZO2) at room temperature, versus  $6 \times 10^{-4}$  for ZnO<sub>1-x</sub> (sample ZO3). A possible explanation is that the actual Al-doping of the crystallites of the film is less than the Al proportion in the target. A ZnO/CuPc/Au photovoltaic structure was fabricated, showing a value of the external quantum efficiency of 12% at its maximum. However, that structure needs to be improved to increase its optical efficiency and charge collection.

## REFERENCES

1. T. Minami, H. Sonohara, T. Kakumu, S. Takata, *Thin Solid Films*, **270**, 37 (1995).
2. H. L. Ma, D. H. Zhang, P. Ma, S. Z. Win, S. Y. Li, *Thin Solid Films*, **263**, 105 (1995).
3. K. Utsumi, O. Matsunaga, T. Takahata, *Thin Solid Films*, **334**, 30 (1998).
4. S. H. Jeong, S. Kho, D. Jung, S. B. Lee, J. -H. Boo, *Surf. Coat. Tech.*, **174-175**, 187 (2003)
5. H. Kim, J.S. Horwitz, W.H. Kim, A.J. Makinen, Z.H. Kafafi, D.B. Crisey, *Thin Solid Films*, **420-421**, 539 (2002).
6. T. Miyata, Y. Minamino, S. Ida, T. Minami, *J. Vac. Sci. Technol.*, **A22**, 1711 (2004).
7. M. -M. Bagheri-Mohagheghi, M. Shokooh-Saremi, *Thin Solid Films*, **441**, 238 (2003).
8. S.-Y. Lee, B.-O. Park, *Thin Solid Films*, **510**, 154 (2006).
9. W.Y. Liang, A.D. Yoffe, *Phys. Rev. Lett.*, **20**, 59 (1968).
10. K. Ellmer, *J. Phys. D: Appl. Phys.*, **34**, 3097 (2001).
11. D.C. Reynolds, D.C. Look, B. Jogai, *J. Appl. Phys.*, **89**, 6189 (2001).
12. T.-B. Hur, Y.-H. Hwang, H.-K. Kim, *J. Appl. Phys.*, **96**, 1507 (2004).
13. D.H. Zhang, H.L. Ma, *Appl. Phys.* **A62**, 487 (1996).
14. A. Anselm, *Introduction to Semiconductor Theory* (Mir Publishers, Moscow, 1981), p. 490.
15. S.B. Zhang, S.-H. Wei, A. Zunger, *Phys. Rev.* **B63**, 075205 (2001).
16. D. C. Look, J. W. Hemsky, J. R. Sizelove, *Phys. Rev. Lett.* **82**, 2552 (1999).